

A Role for *c-myc* in Chemically Induced Renal-Cell Death

YI ZHAN,¹ JOHN L. CLEVELAND,^{2,3} AND JAMES L. STEVENS^{1*}

W. Alton Jones Cell Science Center, Lake Placid, New York 12946¹; St. Jude Children's Research Hospital, Department of Biochemistry, Memphis, Tennessee 38105²; and Department of Biochemistry, University of Tennessee, Memphis, Tennessee 38163³

Received 2 July 1997/Returned for modification 17 August 1997/Accepted 29 August 1997

A variety of genes, including *c-myc*, are activated by chemical toxicants in vivo and in vitro. Although enforced *c-myc* expression induces apoptosis after withdrawing survival factors, it is not clear if activation of the endogenous *c-myc* gene is an apoptotic signal after toxicant exposure. The renal tubular epithelium is a target for many toxicants. *c-myc* expression is activated by tubular damage. In quiescent LLC-PK1 renal epithelial cells, *c-myc* but not *max* or *mad* mRNA is induced by the nephrotoxicant *S*-(1,2-dichlorovinyl)-L-cysteine (DCVC). The kinetics of DCVC-induced *c-myc* expression and apoptosis suggested an association between cell death and prolonged activation of *c-myc* expression after toxicant exposure. Accordingly, prolonged activation of an estrogen receptor-Myc fusion construct, but not a construct in which a c-Myc transactivation domain had been deleted, was sufficient to induce apoptosis in LLC-PK1 cells. Moreover, under conditions in which necrosis was the predominant cell death pathway caused by DCVC in parental cells, overexpressing *c-myc* biased the cell death pathway toward apoptosis. DCVC also induced ornithine decarboxylase (*odc*) mRNA and activated the *odc* promoter. Activation of the *odc* promoter by DCVC required consensus c-Myc-Max binding sites in *odc* intron 1. Inhibiting ODC activity with α -difluoromethylornithine delayed DCVC-induced cell death. Therefore, *odc* is a target gene in the DCVC apoptotic pathway involving *c-myc* activation and contributes to apoptosis. Finally, a structurally related cytotoxic but nongenotoxic analog of DCVC did not induce *c-myc* and did not activate the *odc* promoter or induce apoptosis. The data support the hypothesis that activation of apoptotic cell death in quiescent renal epithelial cells involves induction of *c-myc*. This is the first study to demonstrate that *c-myc* induction by a specific nephrotoxicant leads to gene activation and cell death.

c-Myc is a nuclear transcription factor that functions as a master regulator of the cell cycle and thus regulates proliferation, differentiation, neoplasia, and cell death; the role of *c-myc* in these processes has been reviewed elsewhere (8, 44, 50). The *c-myc* mRNA encodes two short-lived phosphoproteins initiated at independent CUG and AUG translational start sites (25). c-Myc is the prototypical member of a family of DNA binding proteins that contain carboxy-terminal basic helix-loop-helix leucine zipper (bHLH-LZ) domains (8). The transcriptional activity of c-Myc requires dimerization with Max, another member of the family; these heterodimers bind specifically to CACGTG sites in DNA (10, 37). c-Myc harbors N-terminal transcriptional activation domains. c-Myc-Max heterodimers preferentially activate transcription (34, 35). By contrast, Max also forms homodimers that bind CACGTG motifs but do not activate transcription (24). Transactivation by Myc-Max heterodimers is modulated by phosphorylation or binding of p107, a protein related to the retinoblastoma gene product, to the N terminus of c-Myc (5, 7, 23). Max also forms dimers with at least four other bHLH-LZ proteins, which are termed Mad-1, -3, -4, and Mxi-1 (2, 31, 72). Mads-Max heterodimers bind the same consensus sequence (CACGTG) as Myc-Max heterodimers, and yet they repress rather than activate transcription, an effect that requires their interaction with the generalized transcriptional repressor Sin3 (3, 56). Thus, changes in the steady-state levels of activating c-Myc-Max heterodimers and ternary repressor complexes of Sin3-Mad-

Max apparently regulate the expression of genes critical for progression through the cell cycle.

c-myc was identified as a proto-oncogene and immediate-early response gene and, thus, attention initially focused on its role in the cell cycle (8, 44, 50). However, enforced expression of *c-myc* augments the apoptotic program, and thus, rapid cell death occurs when cells are deprived of survival factors (1, 19, 27). In addition, c-Myc also plays an active role in cell death caused by environmental stresses including viral infection, T-cell receptor activation, tumor necrosis factor, and chemotherapeutic agents (4, 12, 15, 32, 33, 36, 39, 58). Apoptosis induced by enforced *c-myc* expression requires a functional transactivation domain indicating that activation of gene targets is necessary (19, 38). c-Myc targets include the ornithine decarboxylase (*odc*), *p53*, and *cdc25A* genes (6, 21, 49, 53, 54, 68). Increased ODC activity leads to increased superoxide levels as a consequence of polyamine metabolism, suggesting that oxidative stress may be involved in c-Myc-induced apoptosis (49). However, direct measurement of reactive oxygen species in cells overexpressing *c-myc* failed to detect elevated levels (48). Nonetheless, inhibiting ODC attenuates but does not prevent apoptosis in *c-myc*-overexpressing myeloid cells (49). *cdc25A* is a phosphatase that activates cyclin-dependent kinases (Cdks) essential for a G₁-to-S transition, and its expression is induced by c-Myc (21). In fibroblasts, overexpressing *cdc25A* augments apoptosis induced by serum deprivation and suppressing *cdc25A* blocks apoptosis induced by enforced *c-myc* expression (21). Although the connection between apoptosis and induction of *p53* and/or *c-myc* is less clear (50, 55, 67), the role of *p53* in apoptosis is well known (41); *p53* is required for c-Myc-induced apoptosis of some cell types (29, 67). Thus, the data

* Corresponding author. Mailing address: W. Alton Jones Cell Science Center, Old Barn Rd., Lake Placid, NY 12946. Phone: (518) 523-1253. Fax: (518) 523-1849. E-mail: jstevens@northnet.org.

strongly support the idea that transcriptional activation of target genes is essential for c-Myc-induced apoptosis.

Both enforced *c-myc* expression and treatment with chemical toxicants cause apoptosis. However, there are remarkably few studies that critically address the role of endogenous *c-myc* expression in apoptosis initiated by toxicants. However, the fact that *c-myc* mRNA is induced in vivo and in cells in culture by a variety of environmental stresses including cytokines, ionizing or UV irradiation, heavy metals, oxidative stress, and chemicals (13, 14, 43, 59, 61, 71) suggests that this may be the case. This connection is strengthened by the observations that expression of *bcl-2* or, in some but not all cases, mutant *p53* blocks apoptosis induced by *c-myc* overexpression and by a variety of toxicants, cytokines, and other stressful insults (30, 40, 41, 47, 57, 62, 66). Together, therefore, these data support the idea that *c-myc* expression contributes to apoptosis induced by physiological and environmental stress. Nevertheless, convincing evidence linking activation of the endogenous *c-myc* gene with apoptosis induced by chemicals is lacking.

c-myc mRNA levels increase in the kidney in vivo and in kidney epithelial cells in vitro after exposure to nephrotoxins (13, 45, 61, 63, 71). Like myeloid and mesenchymal cells, enforced *c-myc* expression induces apoptosis in rat kidney epithelial cells deprived of serum (55), indicating that activation of *c-myc* might play a role in cell death in the renal epithelium. *S*-(1,2-dichlorovinyl)-L-cysteine (DCVC) is a genotoxic metabolite of the environmental and industrial toxicants trichloroethylene and dichloroacetylene (17). The nephrotoxicity of DCVC has been well characterized; cells die after DCVC exposure either by apoptosis or necrosis via pathways involving covalent binding of a reactive metabolite, loss of glutathione, increased levels of cellular Ca^{2+} and reactive oxygen species, disruption of the actin cytoskeleton, and peroxidation of membrane lipids (11, 64, 65). DCVC induces *c-myc* mRNA in a manner that is linked, at least in part, to an increase in cellular Ca^{2+} content and oxidative stress (71). Thus, DCVC is a good model for investigating the role of *c-myc* induction in toxicant-induced cell death. Herein, we present evidence that induction of *c-myc* and its target genes is intimately linked to toxicant-induced cell death and that c-Myc transcriptional activation of target genes biases cell death toward apoptosis over necrosis.

MATERIALS AND METHODS

Materials. Fetal bovine serum and Dulbecco's modified Eagle's medium (DMEM) were purchased from Life Technologies, Inc. (Grand Island, N.Y.). LLC-PK1 cells were purchased from the American Type Culture Collection (Rockville, Md.) at passage 195 and were used between passages 204 and 220. DCVC and *S*-(1,1,2,2-tetrafluoroethyl)-L-cysteine (TFEC) were synthesized as described elsewhere (28). *N,N'*-diphenyl-*p*-phenylenediamine (DPPD) was obtained from Kodak. Tran³⁵S-label containing [³⁵S]methionine and [³⁵S]cysteine was purchased from ICN Biomedicals. α -Difluoromethylornithine (DFMO) was kindly provided by Eckehard Bohme of Marion Merrill Dow Research Laboratories. Benzyloxycarbonyl-Val-Ala-Asp-fluoromethylketone (zVAD.FMK) was purchased from Enzyme Systems Products (Dublin, Calif.). Acetyl-Asp-Glu-Val-Asp-*p*-nitroalanine was purchased from California Peptide Research, Inc. (Napa, Calif.). All other chemicals were obtained from commercial sources and were used without further purification.

Cell culture and toxicant treatment. LLC-PK1 cells were maintained at 37°C in a humidified atmosphere of 95% air and 5% carbon dioxide in DMEM containing 10% fetal bovine serum (complete medium) as described elsewhere (11). Confluent monolayers of LLC-PK1 cells in 6-well or 6.0- or 10-cm dishes were treated with DCVC or TFEC in Earle's balanced salt solution (EBSS) in a final volume of 2.4, 7, or 13 ml, respectively, and then washed twice with phosphate-buffered saline (PBS) and allowed to recover in complete medium. The inhibitors DPPD (20 μ M) and DFMO (10 mM) were added either during toxicant treatment and the recovery period or only during the recovery period, respectively. When cells were treated with amino(oxy)acetic acid (AOA; 100 μ M), it was added 30 min prior to adding the toxicant and then during toxicant treatment.

Cell death assays. Cell death was measured by the release of lactate dehydrogenase (LDH) as described elsewhere (11). The percent cell death was calculated

from the amount of LDH release caused by toxicant treatment relative to that released by 0.1% Triton X-100, i.e., 100% release. When DNA ladder formation was determined, cells were scraped from 60-mm dishes into the medium and harvested by centrifugation. The supernatant was used to measure LDH release. The cell pellet was lysed in buffer containing 10 mM Tris (pH 8.0), 2 mM EDTA, and 0.2% Triton X-100 and incubated on ice for 10 min. Cell debris was removed by centrifugation at 14,000 rpm for 15 min at 4°C. The soluble DNA sample was treated with RNase (60 μ g/ml) for 1 h at 37°C and then with proteinase K (120 μ g/ml) in 0.5% sodium dodecyl sulfate (SDS) for 1 h at 50°C. The DNA was precipitated by adding an equal volume of isopropanol and separated by electrophoresis on 2% agarose gels.

Fragmented nuclei were visualized after staining cells with Hoechst 33258 (64). LLC-PK1 cells were grown on glass coverslips coated with collagen. After treatment, the cells were fixed with 3.7% formaldehyde in PBS for 10 min at room temperature. After washing twice with PBS, the cells were permeabilized with methanol (-20°C) for 6 min. The cells were washed again with PBS and incubated with 1 μ g of Hoechst 33258 per ml in PBS for 10 min at room temperature while shaking. Thereafter, the coverslips were washed three times with PBS and mounted for observation with a Nikon episcopic fluorescence microscope. Since cells with fragmented nuclei rapidly detached from the coverslips, nuclear fragmentation was determined within 24 h after DCVC treatment, whereas DNA ladders and LDH release were determined 24 h after initiating DCVC treatment.

Northern analysis, immunoprecipitation, and Western blotting. Poly(A) mRNA was purified with oligo(dT), separated by denaturing agarose gel electrophoresis, and transferred to nitrocellulose paper by standard techniques. A random priming kit (Boehringer Mannheim) was used to label cDNA probes with [³²P]dCTP. Blots were subjected to Northern analysis by standard techniques. The autoradiograms were exposed with one intensifying screen and Dupont Cronex film (Dupont). The full-length human *mad-1* and *max* cDNA probes were obtained from Robert Eisenman. The human *c-myc* cDNA has been referenced elsewhere (6).

³⁵S labeling of LLC-PK1 cells grown in 60-mm dishes was used to detect newly synthesized c-Myc protein. After a 3-h incubation with DCVC, methionine- and cysteine-free DMEM was added for 1 h. Then, cysteine- and methionine-free DMEM containing 400 μ Ci of [³⁵S]methionine and [³⁵S]cysteine (0.36 μ mol) per ml was added for an additional 1 h. The cells were lysed in 1 ml of buffer containing 58 mM Na₂HPO₄, 17 mM NaH₂PO₄, 68 mM NaCl, 1% Triton X-100, 0.5% sodium deoxycholate, and 0.1% SDS (pH 7.3 to 7.4). Myc proteins were immunoprecipitated with a mouse monoclonal anti-Myc antibody (Ab-2; Oncogene Science) and protein A beads. Immune complexes were resuspended in sample preparation buffer and separated by electrophoresis in 8.5% polyacrylamide-SDS gels. The gels were dried and applied to film for fluorography as described above. When cell proteins were immunoblotted, the cells were lysed and boiled directly in sample preparation buffer. Protein concentrations were determined by the Bio-Rad Protein Assay. Equal amounts of the protein (50 μ g) were resolved on 8.5% SDS gels and transferred to nitrocellulose membranes (Micon Separations Inc.). The blots were probed with 0.5 μ g of affinity-purified c-Myc polyclonal antibody per ml from Upstate Biotechnology and developed with the Enhanced Chemiluminescence System (Amersham).

Plasmid construction, cell transfection, and reporter gene analysis. Luciferase reporter constructs of the *odc* promoter containing either the wild-type (i.e., both CACGTG sites intact [pOdcWT]) or mutated (i.e., both sites changed to CACCTG [pOdcMT]) E-box elements were prepared as described elsewhere (51). LLC-PK1 cells were transfected with pOdcWT and pOdcMT by using Lipofectin (Life Technologies). Cells that had integrated the constructs, i.e., pkOdcWT and pkOdcMT cells, respectively, were selected with G418 (800 μ g/ml). After toxicant treatment, the cells were lysed in buffer containing 1% Triton X-100 and 2.5 mM glycylglycine (pH 7.8) and luciferase activity was determined with 100 μ g of cell protein. The human *c-myc* cDNA was subcloned into pcDNA3 (Invitrogen) to create pCmvMyc. LLC-PK1 cells were transfected with pCmvMyc or empty pcDNA3 by using Lipofectin, and cell lines were selected with G418 (800 μ g/ml). Several independent clones expressing *c-myc*, which were designated pkMyc clones 3, -7, and -9, and clones from the empty vector (pcDNA3) pool, which were designated pkNeo clones 1, -3, and -9, were selected by ring cloning.

We also prepared cells that had integrated a pcDNA3-based plasmid encoding a mutant estrogen receptor (ER) fused to either a wild-type *c-myc* cDNA (pkMycER) or *c-myc* with a deletion that encompassed amino acids 106 to 143 (D₁₀₆₋₁₄₃pkMycER) within the transactivating domain. Nuclear translocation of the MycER proteins is sensitive to 4-OH-tamoxifen but not estrogen; thus, the c-Myc activity of the fusion protein can be regulated by the addition of 4-OH-tamoxifen (38). The advantage of this model over a wild-type ER fusion protein is that estrogenic substances found in serum and culture medium do not interfere with activation; thus, c-Myc is off in the presence of normal growth medium.

On a technical note, selecting cells for G418 resistance resulted in a modest but reproducible decrease in sensitivity to DCVC. For example, a 3-h treatment with DCVC was sufficient to kill as much as 50% of the wild-type LLC-PK1 cells, whereas the treatment time was generally extended up to 5 h in pkNeo or pkOdc cells. Thus, different treatment times and DCVC concentrations were used to accommodate these differences in sensitivity; concentrations and treatment times are noted in the legends to the figures. As shown below, pkMyc clones were remarkably sensitive to toxicant treatment.

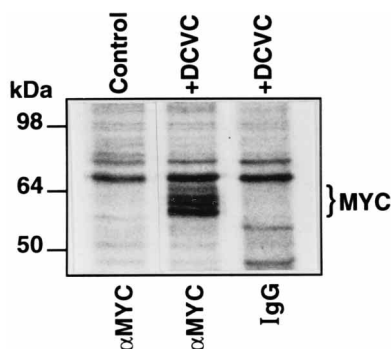


FIG. 1. Myc protein increases after DCVC treatment. After 3 h of treatment with DCVC (0.1 mM), the cells were washed and returned to complete medium for 1 h. A mixture of [35 S]methionine and [35 S]cysteine (400 μ Ci/ml and 0.36 μ mol/ml) was added for 1 h, and labeled cells were scraped. 35 S-labeled proteins were immunoprecipitated with either anti-Myc antibody (α MYC) or a nonspecific immunoglobulin (IgG) and separated on 8.5% gels. Gels were dried for autoradiography (see Materials and Methods). The treatments are indicated at the top of the autoradiogram, and the antibodies used in the immunoprecipitation are listed at the bottom. The data are from a single experiment representative of three separate experiments.

ODC enzyme activity assays. ODC activity was assayed by measuring the release of 14 CO $_2$ from L-[1- 14 C]ornithine (70). The cells were washed twice in PBS and lysed in ice-cold buffer containing 0.5% (vol/vol) Triton X-100, 25 mM Tris-HCl (pH 7.5 at 22°C), 0.1 mM EDTA, and 1 mM dithiothreitol. Cell debris was removed by centrifugation for 5 min at 14,000 rpm at 4°C. L-[1- 14 C]ornithine (0.125 μ Ci; specific activity, 58.0 mCi/mmol; New England Nuclear) was then added to the cell extract. The mixture was incubated at 37°C in a 1-dram (1 fluidram = 3.697 ml) vial. 14 CO $_2$ was trapped on a sodium hydroxide-soaked filter that was held in place above the reaction mixture by a screw cap fitted with a silicone rubber septum. The reaction was terminated by injecting 1 ml of 2 M citric acid through the septum, and the radioactivity trapped on the filter paper was determined by liquid scintillation counting after equilibration in a scintillation cocktail for 48 h.

Statistical analysis. The data are expressed as the means \pm standard deviations. When appropriate, significant differences ($P < 0.05$) were determined either by a one-tailed Student t test or by a one-way analysis of variance (ANOVA) followed by multiple comparisons by the Student Neuman-Keul test. Significant differences are noted in the figures by letter designations or in the figure legends. Data points with one letter designation are significantly different from points with another letter designation; thus, a mean marked A is significantly different from a mean marked B, while a mean marked AB is not different from either A or B.

RESULTS

Kinetics of *c-myc* expression and DCVC-induced apoptosis. DCVC activates the *c-myc* gene in the porcine renal epithelial cell line LLC-PK1 (71). Both *max* and *mad-1* mRNAs were also detected in LLC-PK1 cells; however, neither was induced in response to chemical stress (data not shown). Induction of *c-myc* mRNA by DCVC was accompanied by a dramatic increase in newly synthesized c-Myc protein (Fig. 1). Multiple c-Myc translation products consistent with the presence of phosphorylated and unphosphorylated long and short forms of c-Myc, all of which have slightly different mobilities, were detected (see reference 25 and references therein).

We then compared the kinetics of *c-myc* expression and the onset of cell death. DCVC induces both necrotic and apoptotic cell death, depending on the culture conditions (11, 64, 65). Cells treated with DCVC die 4 to 6 h after treatment, releasing LDH into the medium, but nuclear fragmentation and DNA ladders (see below) are not evident. Antioxidants, such as DPPD, block this necrotic cell death when cells are treated with DCVC concentrations in the range of 0.5 mM (11). However, if the DCVC concentration is increased to 1.0 mM or higher in the presence of DPPD, necrosis is blocked but apoptosis occurs (64). Under these conditions, apoptotic cells ini-

tially excluded trypan blue (reference 64; data not shown) during the time when nuclear fragmentation and DNA laddering first occurred (see below). However, apoptotic cells eventually lose membrane integrity and release LDH (42), although much later than necrotic cells, i.e., 12 to 24 h after DCVC treatment. In addition, in the presence of DPPD, caspase 3 activity in LLC-PK1 cell extracts, as measured by the cleavage of acetyl-Asp-Glu-Val-Asp-*p*-nitroaniline, increased from 62 pmol/min/mg of protein to 302 and 964 pmol/min/mg at 12 and 18 h, respectively, after DCVC treatment along with the appearance of DNA ladders and fragmented nuclei, but there was no increase in the amount of caspase 3 activity in DCVC-treated cells, relative to control cells, in the absence of DPPD (i.e., necrosis conditions). In the presence of the caspase inhibitor zVAD.FMK, cell death caused by DCVC plus DPPD was not significantly different from that for untreated cells ($P < 0.05$; Student's t test; data not shown), while in the absence of zVAD.FMK, cell death was typically 30% (Fig. 2). DNA laddering and nuclear fragmentation were also blocked (data not shown). On the other hand, zVAD.FMK did not block necrotic cell death, i.e., in the absence of DPPD. Therefore, we used DNA ladder formation and nuclear fragmentation (see below) as indicators of apoptosis and LDH release as a quantitative measure of either apoptotic or necrotic cell death (64).

In the presence of DPPD, the maximal increases in c-Myc protein induced by low (0.1 mM) and high (1.5 mM) DCVC concentrations were similar. However, the increase in c-Myc expression after 1.5 mM DCVC was delayed and sustained relative to the rapid rise and decline observed after treatment with 0.1 mM DCVC (Fig. 2B and C). The delayed and sustained increase in c-Myc after treatment with 1.5 mM DCVC correlated temporally with an increase in DNA laddering and cell death (Fig. 2A and D). Therefore, apoptosis induced by treatment with 1.5 mM DCVC correlates with the delayed kinetics of *c-myc* activation as well as the sustained increase in c-Myc protein.

Enforced c-Myc expression sensitizes renal epithelial cells to DCVC-induced apoptotic cell death. If *c-myc* expression contributes to the apoptotic cell death caused by nephrotoxics, then *c-myc* expression should sensitize cells to DCVC. LLC-PK1 cells that had integrated a human *c-myc* gene driven by a cytomegalovirus promoter (pkMyc cells) were prepared by selection in G418. Compared to clones that carried the resistance marker only, i.e., pkNeo-1, -3, and -9 clones, the pkMyc-3, -7, and -9 clones had enhanced levels of human Myc protein that migrated more slowly than the endogenous porcine c-Myc protein (data not shown). Growth of pkMyc cells was accelerated relative to pkNeo cells (data not shown). However, in the presence of complete medium, both pkNeo and pkMyc cells formed confluent monolayers with domes (Fig. 3), which are characteristic of renal epithelial cells (26, 60). When pkNeo cells were treated with a moderate concentration of DCVC (0.5 mM) for 0, 4, 6, and 8 h and returned to complete medium in the presence of DPPD to prevent necrosis (11), cell death was completely blocked. By contrast, pkMyc-3, -7, and -9 cells detached and died with a concomitant appearance of DNA ladders and fragmented nuclei (Fig. 3). Notably, serum withdrawal did not induce apoptosis in confluent pkMyc-7 cells under the conditions used for DCVC treatment (data not shown).

We also determined if *c-myc* expression increased the sensitivity of LLC-PK1 cells to necrotic cell death, i.e., DCVC treatment in the absence of DPPD. Under these conditions, pkNeo and pkMyc-7 cells were equally sensitive to DCVC-induced cell death (Fig. 4). However, DNA ladders and fragmented nuclei were present only in pkMyc-7 cells after treat-

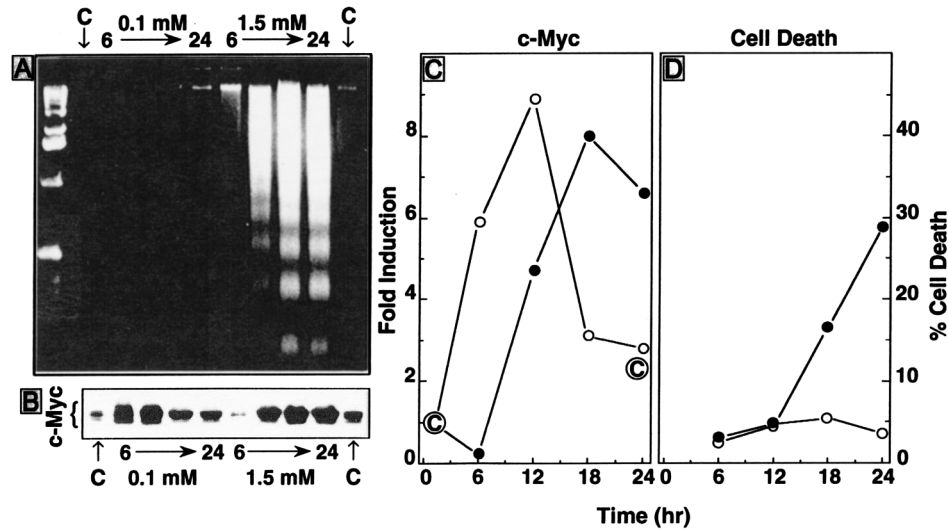


FIG. 2. Analysis of c-Myc protein, DNA fragmentation, and cell death following DCVC treatment. Confluent cultures were exposed to either 0.1 or 1.5 mM DCVC for 6 h in the presence of the antioxidant DPPD and then returned to DMEM supplement with 10% fetal bovine serum and DPPD. Cells were harvested by scraping and centrifugation 6, 12, 18, and 24 h after initiating DCVC treatment and processed for DNA fragmentation, Western blotting, and cell death determinations. (A) DNA collected at 6, 12, 18, and 24 h subjected to agarose gel electrophoresis and stained with ethidium bromide. A 1-kb DNA ladder is shown on the far left. Control cells, treated with EBSS alone for 6 h, were harvested immediately or 24 h later; C, control lanes (on the left, 6-h control; on the right, 24-h control). Control samples were not collected at the other time points. (B) Protein samples collected from cells treated as described above and immunoblotted for c-Myc. (C) The blot shown in panel B quantitated by scanning densitometry. Integrated optical densities of the bands were converted to fold increases in c-Myc protein relative to the integrated optical density at 6 h. The circled C shown at 0 and 24 h indicates the c-Myc protein contents detected in cells 6 and 24 h after initiating treatment with EBSS alone. The 6-h value is used as the zero time control since c-Myc protein levels do not change remarkably between 6-h-vehicle (EBSS)-treated cells and cells harvested immediately from complete medium. (D) The percent cell death determined after treatment with 0.1 or 1.5 mM DCVC as described above. In panels C and D, the open and closed circles are data from 0.1 and 1.5 mM DCVC, respectively. The data shown are from one experiment in which all of the measurements were made with a single set of samples but are representative of three separate experiments.

ment with DCVC. These cells became round and detached, which is characteristic of apoptotic cell death. Although cell death was equivalent in DCVC-treated pkNeo cells, neither DNA ladders nor nuclear fragmentation occurred and the cell corpses remained attached to the dish (Fig. 4). Thus, enforced *c-myc* expression not only sensitizes cells to apoptotic cell death after chemical treatment but also biases the mode of cell death toward apoptosis.

An analog of DCVC that fails to activate *c-myc* does not kill LLC-PK1 cells by apoptosis. To determine if ablating *c-myc* induction altered the kinetics or mode of cell death following DCVC treatment, we attempted to modulate c-Myc levels after toxicant treatment by expressing antisense *c-myc* RNA or dominant-negative c-Myc proteins or by adding phosphorothioate antisense oligonucleotides. Expression of antisense RNA to *c-myc* or a dominant-negative c-Myc protein was toxic in all cases, while antisense oligonucleotides were ineffective in modulating c-Myc protein levels, perhaps due to the high levels of extracellular hydrolases on the brush border membrane of renal epithelial cells. Therefore, we took a chemical approach. *S*-(1,1,2,2-tetrafluoroethyl)-*L*-cysteine (TFEC) is a nephrotoxic but nongenotoxic analog of DCVC that is activated to a reactive acylating species by the same enzyme system that activates DCVC (22). Both compounds cause necrotic cell death in LLC-PK1 cells (see below) with similar biochemical characteristics (11, 38a, 65). However, TFEC did not induce c-Myc protein (Fig. 5). The apparent loss of c-Myc with the higher concentrations of DCVC is due to the shift in the time course of c-Myc expression described above (Fig. 2). Unlike DCVC, TFEC was equally toxic to pkMyc and pkNEO cells (see Fig. 9 below for a comparison of cell death data with DCVC and TFEC), in the presence or absence of DPPD, but did not cause DNA laddering (Fig. 5) or nuclear fragmentation (data not

shown) in pkMyc-7 cells. Thus, a structurally related toxic analog of DCVC that did not activate *c-myc* expression did not induce apoptosis, again suggesting that *c-myc* activation is a signal for chemically induced apoptosis in renal epithelial cells.

Transcription is required for c-Myc-induced apoptosis in LLC-PK1 cells. We then determined if c-Myc transcriptional activating activity was necessary for c-Myc to induce cell death in LLC-PK1 cells. Moreover, since the pkMyc cells were able to form confluent monolayers in complete medium, it was unclear if an abrupt activation of c-Myc, which occurred after toxicant treatment, was sufficient in and of itself to induce apoptosis. Therefore, we generated cells in which c-Myc transcriptional activating activity could be controlled by selecting cells that had incorporated a cDNA encoding a wild-type (pkMycER) or a transcriptionally inactive ($D_{106-143}$ pkMycER) c-Myc (from which amino acids 106 to 143 were deleted and which was fused to a 4-OH-tamoxifen-regulated murine ER mutant) (see Materials and Methods). Addition of 4-OH-tamoxifen to confluent pkMycER cells (clone TM15) resulted in DNA fragmentation, while cells became round and detached from the dishes, which is typical of apoptosis (Fig. 6; data not shown). These effects occurred in the presence of serum and in the absence of toxicant. However, addition of 4-OH-tamoxifen to $D_{106-143}$ pkMycER cells (Fig. 6), which carried the transcriptionally inactive ER-Myc fusion gene, did not cause apoptosis. Thus, an intact transcriptional activation domain is necessary for c-Myc-induced apoptosis in LLC-PK1 renal epithelial cells. However, unlike cells that have been selected to constitutively overexpress c-Myc, prolonged activation of the c-Myc-ER chimera by addition of 4-OH-tamoxifen to pkMycER cells was sufficient in and of itself to induce apoptosis in confluent monolayers.

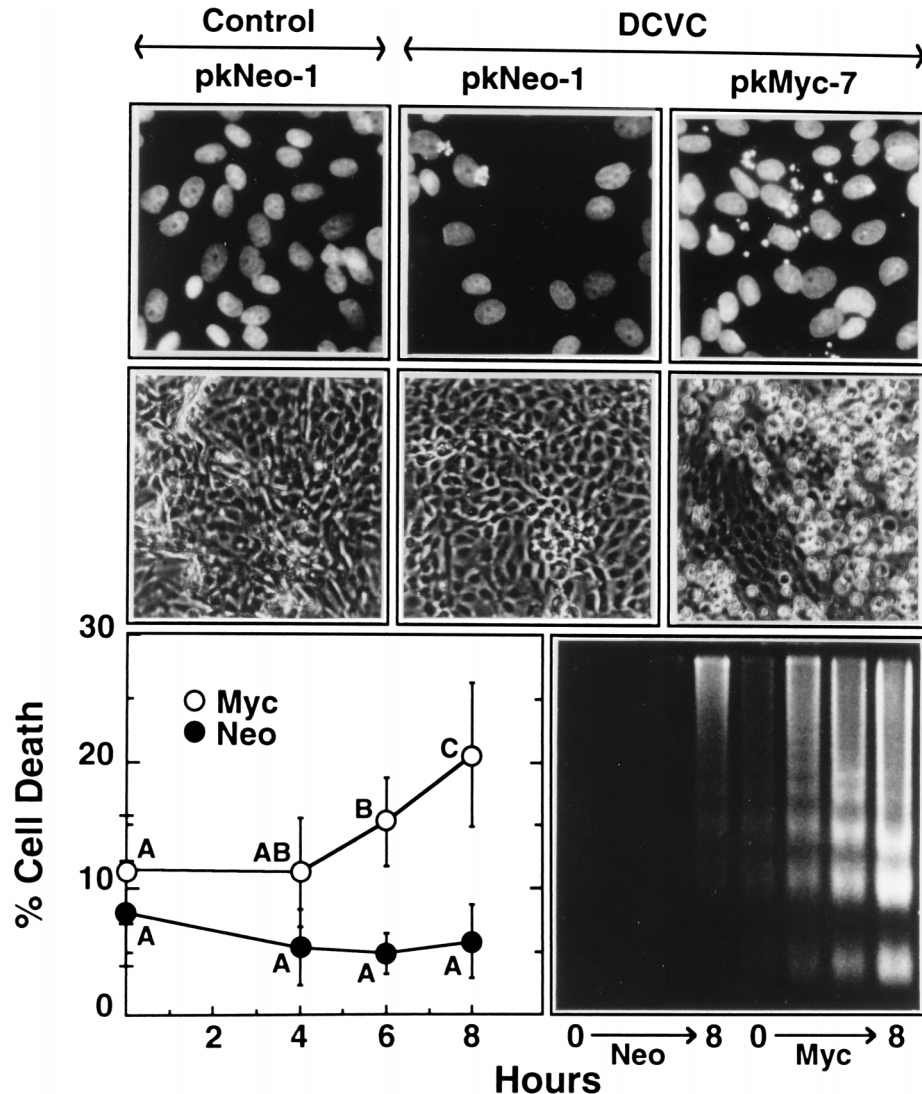


FIG. 3. Enforced expression of c-Myc sensitizes cells to DCVC-induced apoptosis. pkNeo and pkMyc cells were exposed to 0.5 mM DCVC in the presence of DPPD for 0, 4, 6, and 8 h and then returned to completed medium plus DPPD through 24 h after initiating treatment. The times on the abscissa indicate the duration of DCVC treatment; with the exception of Hoechst dye staining (see below), all of the data were gathered 24 h after initiating DCVC treatment. By either phase-contrast or fluorescence microscopy (Hoechst dye staining), there were no discernible differences in morphology between untreated pkNeo and pkMyc cells (control); thus, only a photograph of the pkNeo cells is shown. Morphological analyses by either Hoechst dye or phase-contrast microscopy and DNA ladders were performed with the representative clones pkMyc-7 and pkNeo-1; however, cell death was determined in three independent pkNeo and pkMyc clones. (Top panels) Nuclear morphology after Hoechst dye staining of pkNeo-1 and pkMyc-7 cells before and after DCVC treatment. Cells grown on glass coverslips were fixed 10 min after DCVC treatment for analysis of nuclear morphology by fluorescence microscopy. Once nuclear fragmentation had begun, cells were rapidly released from the coverslips. Note the increased clusters of brightly staining nuclear fragments seen in the pkMyc-7 cells after DCVC treatment. (Middle panels) Phase-contrast photographs of pkNeo-1 and pkMyc-7 cells in culture before and 24 h after DCVC treatment. In the far left panel, a small dome is apparent in control cells. On the far right, many floating cells typical of apoptosis are seen in pkMyc-7 cells. Note that in the presence of DPPD, pkNeo-1 cells treated with DCVC show a normal morphology by phase-contrast and fluorescence microscopy, since the antioxidant blocks cell death completely at this concentration of DCVC (see text). (Lower panels) On the left side, the percent cell death (means \pm standard deviations) determined for three pkMyc clones (clones 3, 7, and 9) in five separate experiments ($n = 5$) is shown. Letter designations indicate significant differences ($P < 0.05$) among the groups as determined by one-way ANOVA (see Materials and Methods). On the right side, representative DNA ladders, collected 24 h after initiating DCVC treatment, are shown for pkNeo-1 (left four lanes) and pkMyc-7 (right four lanes) cells that had been treated with DCVC for 0, 4, 6, or 8 h (indicated by 0 \rightarrow 8 h).

Activation of *ODC* by DCVC is dependent on c-Myc. Since *c-myc* mRNA has been reported to increase in vivo and in vitro after toxicant exposure in previous studies (13, 14, 43, 59, 61, 71) and because c-Myc transcriptional activation was required to induce apoptosis in LLC-PK1 cells, one would predict that induction of apoptosis by DCVC might require activation of *c-myc* target genes. The murine *odc* gene is activated by two conserved CACGTG binding sites for c-Myc-Max located in the first intron (6). Therefore, we determined if there was a

temporal association between *c-myc* and *odc* mRNA induction and if DCVC treatment activated *odc* expression through the CACGTG binding sites. Induction of *odc* mRNA after DCVC treatment followed the increase in *c-myc* mRNA (Fig. 7). In addition, *odc* mRNA levels remained elevated after *c-myc* mRNA had begun to decrease, perhaps due to differences in the half-lives for the mRNAs. ODC activity increased by more than 50-fold and in parallel with the increase in cell death (data not shown). As expected with this concentration of DCVC,

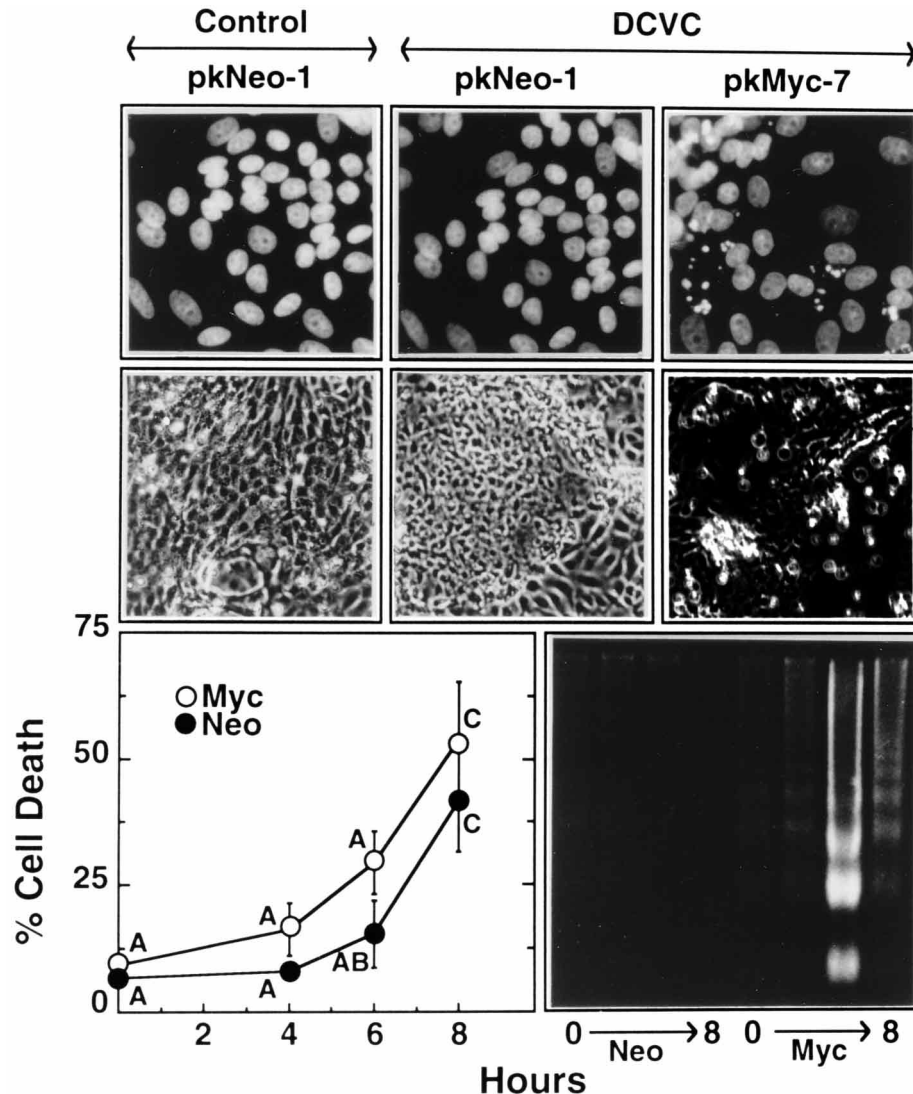


FIG. 4. Enforced expression of c-Myc biases cell death from necrosis to apoptosis. pkNeo and pkMyc clones were exposed to 0.5 mM DCVC for 0, 4, 6, and 8 h in the absence of DPPD and then returned to completed medium, again without DPPD (conditions that favor necrosis [see text]). Data were collected as described in Materials and Methods and the legend to Fig. 3. Nuclear (upper panels) and cellular (middle panels) morphology was inspected by either fluorescence or phase-contrast microscopy, respectively, as described in the legend to Fig. 3. pkMyc-7 cells show evidence of nuclear fragmentation by Hoechst dye staining, and many round floating cells, which are typical of apoptotic death, are present. Note that pkNeo-1 cells remain attached but that patches of necrotic cells are present on the culture surface after DCVC treatment while the pkMyc-7 cells are detached. (Lower panels) In the left panel, cell death data, presented as means \pm standard deviations from three separate experiments with three pkNeo and three pkMyc clonal lines ($n = 3$), are shown for cells treated with DCVC for 0, 4, 6, or 8 h, and percent cell death determined 24 h after initiating DCVC treatment is shown. Letter designations indicate significant differences ($P < 0.05$) among the groups as determined by one-way ANOVA (see Materials and Methods). In the right panel, representative DNA fragmentation patterns for pkNeo-1 cells (left four lanes) and pkMyc-7 cells (right four lanes) treated for 0, 4, 6, and 8 h (0 \rightarrow 8) are shown. After treating pkMyc cells for 8 h with DCVC, they ruptured rapidly and DNA ladders were lost.

DPPD blocked cell death but had no effect on the induction of ODC activity (data not shown).

c-Myc activates a murine *odc* promoter construct in which the two CACGTG sites in the first intron are intact (pOdcWT), but not if they are changed to CACCTG (pOdcMT) (6, 51). Therefore, we prepared LLC-PK1 cells that had integrated either the wild-type or the mutant promoter fused to a luciferase reporter, i.e., pkOdcWT or pkOdcMT cells, respectively. Luciferase activity increased by five- to sixfold in pkOdcWT cells after DCVC treatment but only by two- to threefold in pkOdcMT cells (Fig. 8A). To determine if transcriptional activation of *odc* was in fact a result of DCVC metabolism, we blocked metabolism with AOA, preventing covalent binding of

reactive metabolic fragments (60). AOA treatment abolished pOdcWT activation by DCVC, excluding nonspecific effects of DCVC (Fig. 8B). However, the antioxidant DPPD had no effect on the activation of pOdcWT (Fig. 8B), indicating that pOdcWT activation was associated with conditions that favor apoptotic cell death. Taken together, these data suggest that metabolism of DCVC to a reactive intermediate is required for c-myc expression and activation of *odc* and its promoter.

TFEC did not induce c-Myc protein appreciably (Fig. 5) and failed to activate the *odc* promoter construct (Fig. 9). Stable integration of the pOdcWT construct into the genome did not change the relative sensitivity of LLC-PK1 cells, since both

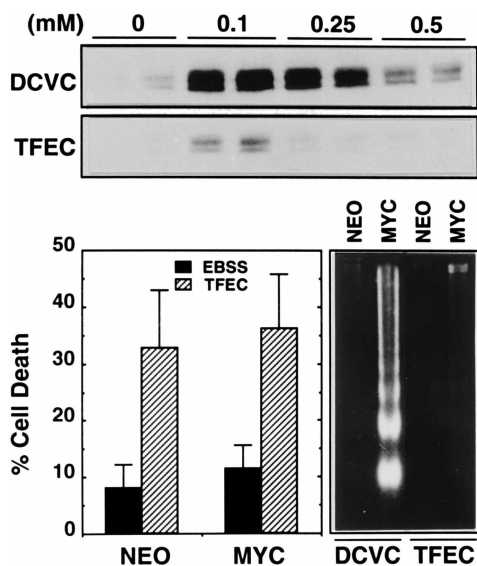


FIG. 5. TFEC, a nongenotoxic analog of DCVC, does not induce *c-Myc* expression, and enforced *c-myc* does not sensitize cells to TFEC. (Top panel) LLC-PK1 cells were treated with increasing concentrations of DCVC or TFEC for 3 h, and samples were collected for immunoblotting with anti-Myc antibody; representative blots are shown. (Middle panel) Three pkMyc clones (clones 3, 7, and 9) and three pkNeo clones (clones 1, 3, and 9) were treated with TFEC (0.5 mM) or DCVC (0.5 mM) in the presence of DPPD for 6 h and then returned to medium containing DPPD. (Left bottom panel) Summary data (means \pm standard deviations) for cell death from three pkNeo and three pkMyc clones 24 h after initiating treatment with EBSS alone or with TFEC. TFEC and DCVC were equally toxic under these conditions (see Fig. 3 and 9 for DCVC data). The data are from three separate experiments with three pkNeo and pkMyc clones ($n = 3$). (Bottom right side) Representative DNA fragmentation patterns for pkNeo-1 (NEO) and pkMyc-7 (MYC) cells treated with 0.5 mM TFEC or DCVC.

DCVC and TFEC remained equally toxic (Fig. 9). Thus, TFEC, the nongenotoxic analog of DCVC, caused only necrosis and was unable to induce *c-Myc* or apoptosis in LLC-PK1 cells and was unable to activate the *odc* promoter, despite the fact that it killed cells by necrosis.

Activation of *ODC* contributes to DCVC-induced cell death. These data indicated that expression of transcriptionally active *c-Myc* protein contributes to toxicant-induced cell death and gene activation in kidney epithelial cells damaged by nephrotoxicants. To determine if *odc* was a functionally important target, we added the ODC inhibitor α -difluoromethylornithine (DFMO) to cells after DCVC treatment and assessed its effect on the rates of cell death. Surprisingly, addition of DFMO caused a modest reduction in release of LDH due to necrosis (Fig. 10). In retrospect, this was not surprising, since activation of ODC enzyme activity occurs prior to either necrotic or apoptotic cell death regardless of whether DPPD is present (Fig. 7, data not shown). In addition, DFMO delayed but did not prevent appearance of DNA ladders (data not shown) and delayed DCVC-induced apoptosis (Fig. 10). These data suggest that the *odc* gene is a target for *c-Myc* transcriptional activation after DCVC treatment and that increased ODC activity contributes, at least partially, to DCVC-induced apoptosis and necrosis.

DISCUSSION

c-myc mRNA levels increase dramatically and remain elevated after treating renal epithelial cells with DCVC (71); therefore, we addressed the role of *c-myc* in the cellular response to toxicant exposure. Herein, we present several lines of

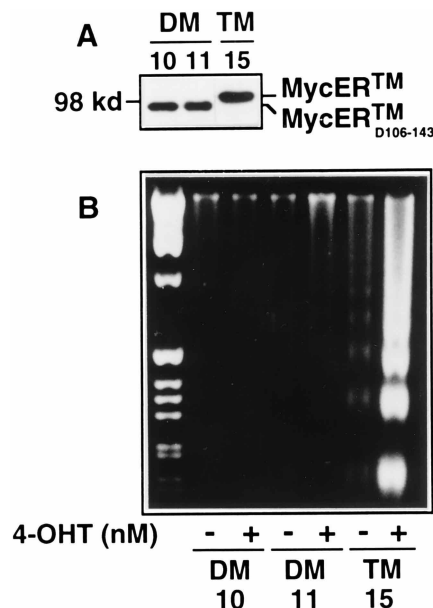


FIG. 6. The transcriptional activation domain of *c-Myc* is necessary for induction of apoptosis. TM15 (clones of LLC-PK1 cells expressing a fusion protein consisting of a 4-OH-tamoxifen-activated ER and *c-Myc* [MycER]) or DM10 and DM11 cells (ER fused to *c-Myc* from which amino acids 106 to 143 had been deleted [_{D106-143}MycER]) were prepared as indicated in Materials and Methods. (A) Equal amounts of cellular protein (50 μ g) were fractionated on an SDS-8.5% polyacrylamide gel and transferred to a nitrocellulose membrane for immunoblot analysis of *c-Myc*. The positions of the (MycER) and (_{D106-143}MycER) proteins are indicated for TM and DM cells. (B) Induction of apoptosis by addition of 4-OH-tamoxifen (4-OHT). One clone of cells expressing the MycER fusion protein (TM15) and two clones of cells expressing the _{D106-143}MycER fusion protein (DM10 and DM11) were cultured for 5 days in the absence of 4-OHT. On day 5, medium was replaced with medium with or without 100 nM 4-OHT. The cells were harvested 24 h after 4-OHT addition for analysis of DNA fragmentation.

evidence that *c-Myc* plays a role in DCVC-induced cell death in LLC-PK1 renal epithelial cells. First, the kinetics of *c-myc* expression correlated with induction of apoptosis. Second, constitutive overexpression of *c-myc* sensitized cells to DCVC-induced apoptosis; remarkably, *c-Myc* also biased the mode of cell death from necrosis to apoptosis. Third, activation of the MycER fusion protein was sufficient to induce apoptosis, and transcriptional activation was a requirement for this response. Fourth, DCVC treatment activated the *c-Myc* transcriptional target *odc* and activated the *odc* promoter reporter construct through a consensus CACGTG binding site present in intron 1, demonstrating that *c-Myc* is a stress-activated transcription factor. Fifth, ODC enzyme activity increased after DCVC treatment, and inhibiting ODC activity delayed renal cell death. Finally, the nongenotoxic homolog TFEC did not activate *c-myc* expression or the *odc* promoter construct and failed to cause apoptosis. Therefore, these data support the idea that DCVC treatment results in activation of *c-Myc* target genes that contribute to apoptotic cell death. To our knowledge, this is the first demonstration that induction of *c-myc* mRNA and protein in response to an environmental insult leads to transcriptional activation of target genes during stress and that transcriptional activation by *c-Myc* is linked to cell death caused by a nephrotoxic chemical.

DPPD stabilizes the plasma membrane after toxicant treatment (11, 65), preventing necrosis but not apoptosis (64). Thus, membrane integrity is a key factor in whether apoptosis occurs (46). We purposely used concentrations of DCVC that could induce either necrosis or apoptosis and then controlled

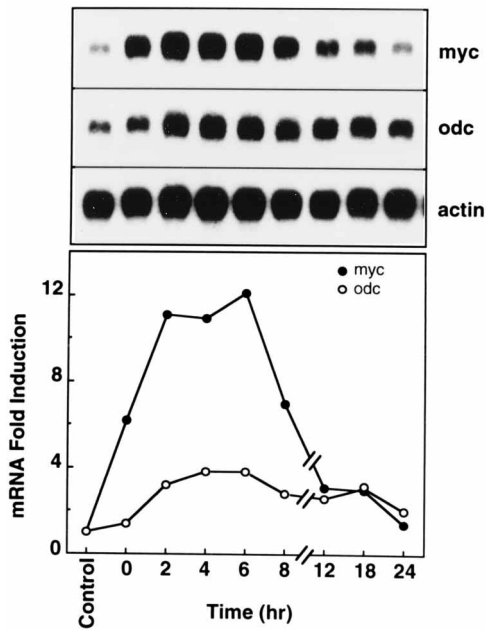


FIG. 7. Induction of *myc* and *odc* mRNA following DCVC treatment. LLC-PK1 cells were treated for 3 h with either EBSS (control) or 0.5 mM DCVC and then washed (0 h) and returned to normal medium. At various times, the cells were harvested and poly(A) RNA was prepared for Northern analysis. The blots were probed with *odc*, *myc*, and β -actin cDNAs. The data were quantified by densitometry, and the *myc* or *odc* mRNA data were normalized to actin. The normalized data are presented in the bottom panel as the fold increases of mRNA compared to cells treated with EBSS alone (control). The data are from a single experiment.

the outcome by adding DPPD in order to evaluate the effects of *c-myc* expression on both pathways. Interestingly, following DCVC treatment, enforced *c-myc* expression biased cell death toward apoptosis under conditions in which apoptosis and apoptotic markers were absent in parental cells (Fig. 6). Thus, *c-Myc* may control a switch point which lowers the threshold for activation of apoptosis. In pkMyc cells, in which the switch is already activated, the damage threshold at which DCVC preferentially induces apoptosis is decreased. Alternatively, *c-Myc* may not control the switch directly, but the threshold for activating the switch is decreased in pkMyc cells. Regardless, *c-myc* expression not only sensitizes cells to apoptotic cell death but also alters the balance between apoptosis and necrosis after toxicant treatment.

Although the signaling pathway that couples DCVC exposure to *c-myc* expression and apoptosis is not clear, the biochemical signals that cause cell death after DCVC exposure are known. The amount of intracellular calcium increases quickly, followed by an increase in mitochondrial oxidant production, membrane peroxidation, and cell lysis (11, 65). Accordingly, chelating cellular Ca^{2+} , adding an iron chelator to block generation of hydroxyl radicals, or adding an antioxidant to scavenge lipid radicals blocks DCVC-induced necrosis (11, 65). Of these inhibitors, only intracellular Ca^{2+} chelation prevents, albeit only partially, the increase in *c-myc* mRNA activation after DCVC treatment (71). However, in preliminary studies, neither Ca^{2+} nor iron chelators block DCVC-induced apoptosis and chelating Ca^{2+} did not decrease *c-Myc* protein expression, indicating that these perturbations are not dominant components of the signaling pathway leading from DCVC exposure to *c-myc* activation (73). TFEC, a nongenotoxic analog of DCVC, which for all intents and purposes shows similar

behavior to DCVC in the biochemistry of cell injury (38a), did not induce *c-myc* expression, activate the *odc* promoter, or cause apoptosis. Thus, DNA damage may play a role in the apoptotic signaling pathway activated by DCVC, at least within the context of the other biochemical perturbations caused by this compound. However, *c-myc* expression sensitizes cells to some forms of injury but not others (39), indicating that the role for *c-Myc* in apoptosis caused by environmental stress is not universal.

Although these data clearly show that *c-Myc* is transcriptionally active under these stressful conditions, i.e., that the pOdc cWT reporter is activated, at this point we can conclude only that activation of *c-myc* target genes contributes to apoptotic cell death but not that they are master switches. This is in agreement with the data for myeloid cells, in which inhibition of ODC activity with DFMO only partially inhibits *c-Myc*-induced cell death (49). Indeed, given that ODC activity is regulated by both transcriptional and posttranscriptional processes (16) and that ODC activity in LLC-PK1 cells participates in both necrosis and apoptosis (Fig. 10), it is unlikely that activation of a single gene or a transcription factor functions as a master cell death switch following chemical damage. Rather, it seems likely that transcriptional activation of *odc* and other *c-myc* target genes contributes to cell death in cooperation with other biochemical perturbations caused by DCVC. Nonetheless, our data support the idea that *c-Myc* is a stress-activated transcription factor which activates target genes that play a significant role in chemically induced apoptosis.

There are additional notable differences between this and other models of *c-myc*-induced cell death. For example, if *c-Myc* signals DCVC-induced apoptosis, then *bcl-2* might be expected to modulate cell death (9, 20, 69). However, enforced *bcl-2* expression does not block DCVC-induced apoptosis (74). In addition, serum withdrawal had no effect on DCVC-induced apoptosis (data not shown), unlike enforced *c-myc* overexpression models. Both *p53*-dependent and -independent apoptotic pathways contribute to

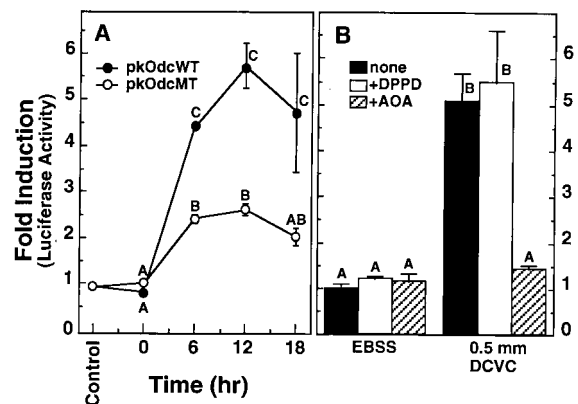


FIG. 8. DCVC treatment activates the ODC promoter via consensus Myc-Max binding sites. (A) pkOdcWT cells and pkOdcMT cells were treated with EBSS (control) or with 0.5 mM DCVC for 5 h, in the absence of DPPD, and returned to normal medium (0 h). Luciferase activities were quantified at various times after DCVC treatment and are expressed as fold increases over activity either in pkOdcWT or pkOdcMT cells which were treated with EBSS alone. The data are the means \pm the ranges of the data from two independent experiments ($n = 2$). Letter designations indicate significant differences among the groups as determined by ANOVA (see Materials and Methods). (B) pkOdcWT cells were treated with EBSS (none) or DCVC (0.5 mM) for 4 h in the presence or absence of the β -lyase inhibitor AOA or the antioxidant DPPD, respectively, and then returned to normal medium containing the inhibitors for another 6 h. The luciferase activities in cell extracts were quantified and are presented as means \pm standard deviations of the fold increases determined from three independent experiments ($n = 3$). In both panels, significant differences ($P < 0.05$) were determined by one-way ANOVA. Means with different letter designations are significantly different.

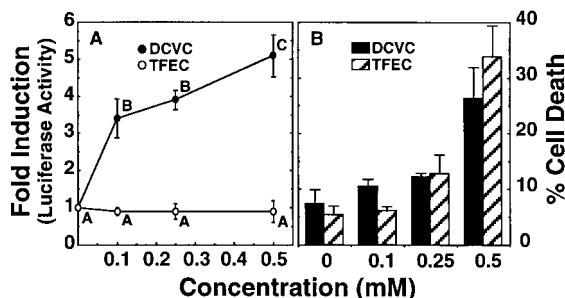


FIG. 9. Activation of the *odc* promoter by DCVC and TFEC. pkOdcWT cells were treated for 4 h with various concentrations of DCVC or TFEC. Samples were collected for analysis of luciferase and percent cell death 10 h after initiating toxicant treatment. The data are the means \pm standard deviations of data collected in three separate experiments ($n = 3$). (A) Fold increase in luciferase activity relative to untreated cells (0 h); (B) LDH release induced by toxicant treatment in pkOdcWT cells treated with TFEC and DCVC. In both panels, significant differences ($P < 0.05$) were determined by one-way ANOVA. In the left panel, means with different letter designations are significantly different ($P < 0.05$). There were no differences detected between cell death induced by DCVC and TFEC at any concentration (B); however, there was a significant increase detected in cell death at the 0.5 mM concentrations of TFEC and DCVC relative to untreated cells.

apoptosis in *c-myc*-overexpressing cells (29, 39, 55), but we have not determined the role of *p53* in DCVC-induced cell death.

Three models have been proposed to explain the role of *c-myc* in apoptosis. The conflict model suggests that conflicting growth signals lead to apoptosis (19). In the dual-signal model, *c-myc* signals apoptosis and cell cycle progression via independent pathways (18). Finally, according to the multiple-effector model, the machinery that controls cell cycle progression and apoptosis overlaps, but cells can sense the apoptosis signal in the absence of cell

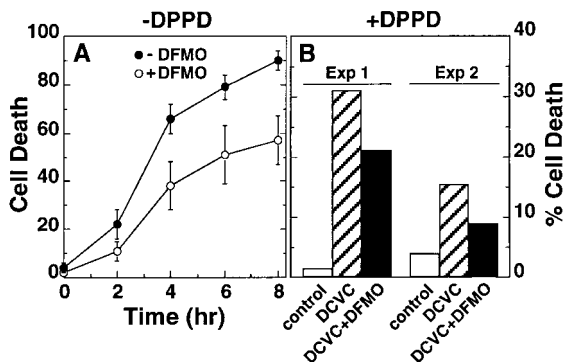


FIG. 10. Inhibition of ODC partially blocks DCVC-induced cell death. (A) LLC-PK1 cells were treated with DCVC (0.25 mM) for 3 h and returned to complete medium with (+) or without (-) DFMO in the absence of DPPD, i.e., under necrosis conditions. The data shown are the means \pm standard deviations of data accumulated from five experiments. DFMO treatment produced a significant decrease ($P < 0.05$) in cell death at all time points shown, as determined by the one-tailed Student *t* test. In general, DFMO was ineffective at higher concentrations of DCVC. Because the cell death at 18 h varied from 50 to 80%, the data were normalized to a percent of the maximum cells death achieved by 24 h in a given experiment; thus, the ordinate is labeled as cell death rather than % cell death (as in panel B). This maneuver revealed that DFMO caused a statistically significant decrease in cell death. (B) The effect of DFMO on cell death in the presence of DPPD, i.e., the apoptosis condition. Cells were treated with EBSS (control) or with 1.0 mM DCVC plus DPPD for 6 h and then returned to DMEM in the presence of DPPD with DFMO (DCVC + DFMO) or without DFMO (DCVC). Cell death was quantitated 24 h after initiating DCVC treatment. The data in panel B are from two individual experiments; thus, standard deviations are not shown. Although the same effect was seen in both experiments, the amounts of cell death varied sufficiently so as to prevent summarizing the data even when the data were normalized as for panel A. Exp, experiment.

cycle progression (52). Because DCVC arrests cell growth (data not shown) and since serum withdrawal has no effect on DCVC-induced apoptosis, the conflict model does not fit the data. Although we cannot exclude the dual-signal model per se based on the *odc* data alone, the multiple-effector model seems to fit the observations best, although additional experiments will be required to substantiate this conjecture. Regardless, it is likely that transcriptional activation of *c-Myc* target genes, be they *odc*, *p53*, and *cdc25A* (21, 49, 54), plays a role in DCVC-induced apoptosis. It will be interesting to determine the generality of this mechanism in apoptosis induced by environmental insults to renal epithelial cells and other cell types.

ACKNOWLEDGMENTS

We thank Daniel Sussman, Jeff Ross, Bob van de Water, Denry Sato, Martin Tenniswood, Susan Jaken, and Steven Goodrich for helpful advice and technical comments. We also thank members of our laboratories for helpful discussion during the course of the work. We acknowledge Jason North for synthesis of DCVC and TFEC as well as the generous contribution of reagents by Eckehard Bohme of Marion Merrill Dow, Trevor Littlewood, Gerard Evan, and Robert Eisenman.

These studies were supported by PHS grants ES07847 (J.L.S.), DK46267 (J.L.S.), and DK44158 (J.L.C.) and by the American Lebanese Syrian Associated Charities (ALSAC).

REFERENCES

1. Askew, D. S., R. A. Ashmun, B. C. Simmons, and J. L. Cleveland. 1991. Constitutive *c-myc* expression in an IL-3-dependent myeloid cell line suppresses cell cycle arrest and accelerates apoptosis. *Oncogene* 6:1915-1922.
2. Ayer, D. E., L. Kretzner, and R. N. Eisenman. 1993. Mad: a heterodimeric partner for Max that antagonizes Myc transcriptional activity. *Cell* 72:211-222.
3. Ayer, D. E., Q. A. Lawrence, and R. N. Eisenman. 1995. Mad-Max transcriptional repression is mediated by ternary complex formation with mammalian homologs of yeast repressor Sin3. *Cell* 80:767-776.
4. Basu, A., and J. S. Cline. 1995. Oncogenic transformation alters cisplatin-induced apoptosis in rat embryo fibroblasts. *Int. J. Cancer* 63:597-603.
5. Beijersbergen, R. L., E. M. Hijmans, L. Shu, and R. Bernards. 1994. Interaction of *c-Myc* with the pRb-related protein p107 results in inhibition of *c-Myc*-mediated transactivation. *EMBO J.* 13:4080-4086.
6. Bello-Fernandez, C., G. Packham, and J. L. Cleveland. 1993. The ornithine decarboxylase gene is a transcriptional target of *c-myc*. *Proc. Natl. Acad. Sci. USA* 90:7804-7808.
7. Berberich, S. J., and M. D. Cole. 1992. Casein kinase II inhibits the DNA-binding activity of Max homodimers but not Myc/Max heterodimers. *Genes Dev.* 6:166-176.
8. Bernards, R. 1995. Flipping the Myc switch. *Curr. Biol.* 5:859-861.
9. Bissonnette, R. P., F. Echeverri, A. Mahboubi, and D. R. Green. 1992. Apoptotic cell death induced by *c-myc* is inhibited by *bcl-2*. *Nature* 359:552-554.
10. Blackwood, E. M., and R. N. Eisenman. 1991. Max: a helix-loop-helix zipper protein that forms a sequence-specific DNA-binding complex with Myc. *Science* 251:1211-1217.
11. Chen, Q., T. W. Jones, P. C. Brown, and J. L. Stevens. 1990. The mechanism of cysteine conjugate cytotoxicity in renal epithelial cells. Covalent binding leads to thiol depletion and lipid peroxidation. *J. Biol. Chem.* 265:21603-21611.
12. Cherney, B. W., K. Bhatia, and G. Tosato. 1994. A role for deregulated *c-Myc* expression in apoptosis of Epstein-Barr virus-immortalized B cells. *Proc. Natl. Acad. Sci. USA* 91:12967-12971.
13. Cowley, B. D., L. J. Chadwick, J. J. Grantham, and J. P. Calvet. 1989. Sequential protooncogene expression in regenerating kidney following acute renal injury. *J. Biol. Chem.* 264:8389-8393.
14. Crawford, D., I. Zbinden, P. Amstad, and P. Cerutti. 1988. Oxidant stress induces the proto-oncogenes *c-fos* and *c-myc* in mouse epidermal cells. *Oncogene* 3:27-32.
15. Davidoff, A. N., and B. V. Mendelow. 1993. Puromycin-elicited *c-myc* mRNA superinduction precedes apoptosis in HL-60 leukaemic cells. *Anticancer Res.* 13:2257-2260.
16. Davis, R. H., D. R. Morris, and P. Coffino. 1992. Sequestered end products and enzyme regulation: the case of ornithine decarboxylase. *Microbiol. Rev.* 56:280-290.
17. Dekant, W., S. Vamvakas, M. Koob, A. Kochling, W. Kanhai, D. Muller, and D. Henschler. 1990. A mechanisms of haloalkene-induced renal carcinogenesis. *Environ. Health Perspect.* 88:107-110.
18. Evan, G. I., and T. D. Littlewood. 1993. The role of *c-myc* in cell growth. *Curr. Opin. Genet. Dev.* 3:44-49.
19. Evan, G. I., A. H. Wyllie, C. S. Gilbert, T. D. Littlewood, H. Land, M. Brooks, C. M. Waters, L. Z. Penn, and D. C. Hancock. 1992. Induction of apoptosis

- in fibroblasts by *c-myc* protein. *Cell* **69**:119–128.
20. **Fanidi, A., E. A. Harrington, and G. I. Evan.** 1992. Cooperative interaction between *c-myc* and *bcl-2* proto-oncogenes. *Nature* **359**:554–556.
 21. **Galaktionov, K., X. Chen, and D. Beach.** 1996. Cdc25 cell-cycle phosphatase as a target of *c-myc*. *Nature* **382**:511–517.
 22. **Green, T., and J. Odum.** 1985. Structure/activity studies of the nephrotoxic and mutagenic action of cysteine conjugates of chloro- and fluoroalkenes. *Chem. Biol. Interact.* **54**:15–31.
 23. **Gu, W., K. Bhatia, I. T. Magrath, C. V. Dang, and R. Dalla-Favera.** 1994. Binding and suppression of the Myc transcriptional activation domain by p107. *Science* **264**:251–254.
 24. **Gu, W., K. Cechova, V. Tassi, and R. Dalla-Favera.** 1993. Opposite regulation of gene transcription and cell proliferation by c-Myc and Max. *Proc. Natl. Acad. Sci. USA* **90**:2935–2939.
 25. **Hahn, S. R., M. Dixit, R. C. Sears, and L. Sealy.** 1994. The alternatively initiated c-Myc proteins differentially regulate transcription through a non-canonical DNA-binding site. *Genes Dev.* **8**:2441–2452.
 26. **Halleck, M. M., N. J. Holbrook, J. Skinner, H. Liu, and J. L. Stevens.** 1997. The molecular response to reductive stress in the renal epithelial cell line LLC-PK1: coordinate transcriptional regulation of *gadd153* and *grp78* genes by thiols. *Cell Stress Chaperones* **2**:31–40.
 27. **Harrington, E. A., M. R. Bennett, A. Fanidi, and G. I. Evan.** 1994. c-Myc-induced apoptosis in fibroblasts is inhibited by specific cytokines. *EMBO J.* **13**:3286–3295.
 28. **Hayden, P. J., and J. L. Stevens.** 1990. Cysteine conjugate toxicity, metabolism, and binding to macromolecules in isolated rat kidney mitochondria. *Mol. Pharmacol.* **37**:468–476.
 29. **Hermeking, H., and D. Eick.** 1994. Mediation of c-Myc-induced apoptosis by p53. *Science* **265**:2091–2093.
 30. **Hockenbery, D., G. Nunez, C. Millman, R. D. Schreiber, and S. J. Korsmeyer.** 1990. Bcl-2 is an inner mitochondrial membrane protein that blocks programmed cell death. *Nature* **348**:334–336.
 31. **Hurlin, P. J., C. Queva, P. J. Koskinen, E. Steingrimsson, D. E. Ayer, N. G. Copeland, N. A. Jenkins, and R. N. Eisenman.** 1995. Mad3 and Mad4: novel Max-interacting transcriptional repressors that suppress *c-myc* dependent transformation and are expressed during neural and epidermal differentiation. *EMBO J.* **14**:5646–5659.
 32. **Janicke, R., F. H. H. Lee, and A. G. Porter.** 1994. Nuclear Myc plays an important role in the cytotoxicity of tumor necrosis factor alpha in tumor cells. *Mol. Cell. Biol.* **14**:5661–5670.
 33. **Kang, Y., R. Cortina, and R. R. Perry.** 1996. Role of *c-myc* in tamoxifen-induced apoptosis estrogen-independent breast cancer cells. *J. Natl. Cancer Inst.* **88**:279–284.
 34. **Kato, G. J., J. Barrett, M. Villa-Garcia, and C. V. Dang.** 1990. An amino-terminal c-myc domain required for neoplastic transformation activates transcription. *Mol. Cell. Biol.* **10**:5914–5920.
 35. **Kato, G. J., W. M. Lee, L. L. Chen, and C. V. Dang.** 1992. Max: functional domains and interaction with c-Myc. *Genes Dev.* **6**:81–92.
 36. **Klefsjorn, J., I. Vastrik, E. Saksela, J. Valle, M. Eilers, and K. Alitalo.** 1994. c-Myc induces cellular susceptibility to the cytotoxic action of TNF-alpha. *EMBO J.* **13**:5442–5450.
 37. **Kretzner, L., E. M. Blackwood, and R. N. Eisenman.** 1992. Myc and Max proteins possess distinct transcriptional activities. *Nature* **359**:426–429.
 38. **Littlewood, T. D., D. C. Hancock, P. S. Danielian, M. G. Parker, and G. I. Evan.** 1995. A modified oestrogen receptor ligand-binding domain as an improved switch for the regulation of heterologous proteins. *Nucleic Acids Res.* **23**:1686–1690.
 - 38a. **Liu, H., and J. L. Stevens.** Unpublished data.
 39. **Lotem, J., and L. Sachs.** 1993. Regulation by *bcl-2*, *c-myc*, and *p53* of susceptibility to induction of apoptosis by heat shock and cancer chemotherapy compounds in differentiation-competent and differentiation-defective myeloid leukemic Cells. *Cell Growth Differ.* **4**:41–47.
 40. **Lotem, J., and L. Sachs.** 1995. A mutant *p53* antagonizes the deregulated *c-myc*-mediated enhancement of apoptosis and decrease in leukemogenicity. *Proc. Natl. Acad. Sci. USA* **92**:9672–9676.
 41. **Lowe, S. W., H. E. Ruley, T. Jacks, and D. E. Housman.** 1993. p53-dependent apoptosis modulates the cytotoxicity of anticancer agents. *Cell* **74**:957–967.
 42. **Majno, G., and I. Joris.** 1995. Apoptosis, oncosis and necrosis. An overview of cell death. *Am. J. Pathol.* **146**:3–15.
 43. **Maki, A., I. K. Berezsky, J. Fargnoli, N. J. Holbrook, and B. F. Trump.** 1992. Role of [Ca²⁺] induction of *c-fos*, *c-jun* and *c-myc* mRNA in rat PTE after oxidative stress. *FASEB J.* **6**:919–924.
 44. **Marcu, K. B., S. A. Bossone, and A. J. Patel.** 1992. *myc* function and regulation. *Annu. Rev. Biochem.* **61**:809–860.
 45. **Matsuoka, M., and K. M. Call.** 1995. Cadmium-induced expression of immediate early genes in LLC-PK1 cells. *Kidney Int.* **48**:383–389.
 46. **McCarthy, N. J., M. K. B. Whyte, C. S. Gilbert, and G. I. Evan.** 1997. Inhibition of Ced-3/ICE-related proteases does not prevent cell death induced by oncogenes, DNA damage, or the Bcl-2 homologue Bak. *J. Cell Biol.* **136**:215–227.
 47. **Nunez, G., L. London, D. Hockenberry, M. Alexander, J. P. McKearn, and S. J. Korsmeyer.** 1990. Deregulated *bcl-2* gene expression selectively prolongs survival of growth factor-deprived hemopoietic cell lines. *J. Immunol.* **144**:3602–3610.
 48. **Packham, G., R. A. Ashmun, and J. L. Cleveland.** 1996. Cytokines suppress apoptosis independent of increases in reactive oxygen levels. *J. Immunol.* **156**:2792–2800.
 49. **Packham, G., and J. L. Cleveland.** 1994. Ornithine decarboxylase is a mediator of c-Myc-induced apoptosis. *Mol. Cell. Biol.* **14**:5741–5747.
 50. **Packham, G., and J. L. Cleveland.** 1995. c-Myc and apoptosis. *Biochim. Biophys. Acta* **1242**:11–28.
 51. **Packham, G., and J. L. Cleveland.** Induction of ornithine decarboxylase by IL-3 is mediated by sequential c-Myc-independent and c-Myc dependent pathways. *Oncogene*, in press.
 52. **Packham, G., C. W. Porter, and J. L. Cleveland.** 1996. c-Myc induces apoptosis and cell cycle progression by separable, yet overlapping, pathways. *Oncogene* **13**:461–469.
 53. **Pena, A., C. D. Reddy, S. J. Wu, N. J. Hickok, E. P. Reddy, G. Yumet, D. R. Soprano, and K. J. Soprano.** 1993. Regulation of human ornithine decarboxylase expression by the c-Myc-Max protein complex. *J. Biol. Chem.* **268**:27277–27285.
 54. **Reisman, D., N. B. Elkind, B. Roy, J. Beamon, and V. Rotter.** 1993. c-Myc trans-activates the *p53* promoter through a required downstream CACGTG motif. *Cell Growth Differ.* **4**:57–65.
 55. **Sakamuro, D., V. Eviner, K. J. Elliott, L. Showe, E. White, and G. C. Prendergast.** 1995. c-Myc induces apoptosis in epithelial cells by both p53-dependent and p53-independent mechanisms. *Oncogene* **11**:2411–2418.
 56. **Schreiber-Agus, N., L. Chin, K. Chen, R. Torres, G. Rao, P. Guida, A. I. Skoultschi, and R. A. DePinto.** 1995. An amino-terminal domain of Mxi1 mediates anti-*myc* oncogenic activity and interacts with a homolog of the yeast transcriptional repressor SIN3. *Cell* **80**:777–786.
 57. **Sentman, C. L., J. R. Shutter, D. Hockenberry, O. Kanagawa, and S. J. Korsmeyer.** 1991. bcl-2 inhibits multiple forms of apoptosis but not negative selection in thymocytes. *Cell* **67**:879–888.
 58. **Shi, Y., J. M. Glynn, L. J. Guilbert, T. G. Cotter, R. P. Bissonnette, and D. R. Green.** 1992. Role for *c-myc* in activation-induced apoptotic cell death in T cell hybridomas. *Science* **257**:212–214.
 59. **Shibanuma, M., T. Kuroki, and K. Nose.** 1990. Stimulation by hydrogen peroxide of DNA synthesis, competence family gene expression and phosphorylation of a specific protein in quiescent Balb/3T3 cells. *Oncogene* **5**:1025–1032.
 60. **Stevens, J., P. Hayden, and G. Taylor.** 1986. The role of glutathione conjugate metabolism and cysteine conjugate beta-lyase in the mechanism of S-cysteine conjugate toxicity in LLC-PK1 cells. *J. Biol. Chem.* **261**:3325–3332.
 61. **Tang, N., and M. D. Enger.** 1993. Cd²⁺-Induced c-myc messenger RNA accumulation in NRK-49F cells is blocked by the protein kinase inhibitor H7 but not by HA1004, indicating that protein kinase C is a mediator of the response. *Toxicology* **81**:155–164.
 62. **Tsujimoto, Y.** 1989. Stress-resistance conferred by high level bcl-2 protein in human B lymphoblastoid cell. *Oncogene* **4**:1331–1336.
 63. **Vamvakas, S., and U. Koster.** 1993. The nephrotoxin dichlorovinylcysteine induces expression of the protooncogenes *c-fos* and *c-myc* in LLC-PK(1) cells—a comparative investigation with growth factors and 12-*O*-tetradecanoylphorbolacetate. *Cell Biol. Toxicol.* **9**:1–13.
 64. **van de Water, B., M. Kruidering, and J. F. Nagelkerke.** 1996. Role of F-actin damage and cell detachment in apoptotic cell death of cultured proximal tubular cells. *Am. J. Physiol.* **270**:F593–F603.
 65. **van de Water, B., J. P. Zoetewij, H. J. G. M. de Bont, G. J. Mulder, and J. F. Nagelkerke.** 1994. Role of mitochondrial calcium in the oxidative stress-induced dissipation of the mitochondrial membrane potential: studies in isolated proximal tubular cells using the nephrotoxin 1,2-dichlorovinyl-cysteine. *J. Biol. Chem.* **269**:14546–14552.
 66. **Vaux, D. L., S. Cory, and J. M. Adams.** 1988. *Bcl-2* gene promotes haemopoietic cell survival and cooperates with *c-myc* to immortalize pre-B cells. *Nature* **335**:440–442.
 67. **Wagner, A. J., J. M. Kokontis, and N. Hay.** 1994. Myc-mediated apoptosis requires wild-type p53 in a manner independent of cell cycle arrest and the ability of p53 to induce p21waf1/cip1. *Genes Dev.* **8**:2817–2830.
 68. **Wagner, A. J., C. Meyers, L. A. Laimins, and N. Hay.** 1993. c-Myc induces the expression and activity of ornithine decarboxylase. *Cell Growth Differ.* **4**:879–883.
 69. **Wagner, A. J., M. B. Small, and N. Hay.** 1993. Myc-Mediated apoptosis is blocked by ectopic expression of Bcl-2. *Mol. Cell Biol.* **13**:2432–2440.
 70. **Weiss, J. M., K. J. Lembach, and R. J. Boucek.** 1981. A comparison of ornithine decarboxylase from normal and SV40-transformed 3T3 mouse fibroblasts. *Biochem. J.* **194**:229–239.
 71. **Yu, K., Q. Chen, H. Liu, Y. Zhan, and J. L. Stevens.** 1994. Signaling the molecular stress response to nephrotoxic and mutagenic cysteine conjugates: differential roles for protein synthesis and calcium in the induction of *c-fos* and *c-myc* mRNA in LLC-PK1 cells. *J. Cell Physiol.* **161**:303–311.
 72. **Zervos, A. S., J. Gyuris, and R. Brent.** 1993. Mxi1, a protein that specifically interacts with Max to bind Myc-Max recognition sites. *Cell* **72**:223–232.
 73. **Zhan, Y., and J. L. Stevens.** Unpublished results.
 74. **Zhan, Y., B. van de Water, and J. L. Stevens.** Unpublished results.